pp. 324-330

A principal component analysis based method for the simulation of turbulence-degraded infrared image sequence

Christine BONDEAU*
El-Bay BOURENNANE*
Michel PAINDAVOINE*

Abstract

We present an original method for the simulation of images degraded by atmospheric turbulence. The existing methods allow us to simulate only images that are temporally decorrelated from each other, in the isoplanatic case, or in weak anisoplanatism. Here, we propose a simulation for the case of strong anisoplanatism. Moreover, the temporal aspect has been studied in order to build up a sequence of degraded images, using principal component analysis (PCA). The images obtained clearly show the effects of anisoplanatism and temporal evolution of turbulence.

Mots clés : Traitement image, Propagation atmosphérique infrarouge, Turbulence atmosphérique, Analyse composante principale, Séquence image, Simulation, Variation temporelle.

UNE MÉTHODE BASÉE SUR L'ANALYSE EN COMPOSANTES PRINCIPALES POUR LA SIMULATION DE SÉQUENCES D'IMAGES INFRAROUGES DÉGRADÉES PAR LA TURBULENCE

Résumé

Une méthode originale de simulation d'images dégradées par la turbulence atmosphérique est présentée. Les méthodes existantes ne permettent de simuler que des images temporellement décorrélées les unes des autres, dans le cas de l'isoplanétisme ou du faible anisoplanétisme. Dans cet article, une simulation pour le cas de fort anisoplanétisme est proposée et une étude sur l'aspect temporel du phénomène dans le but de construire une séquence d'images dégradées, à l'aide de l'analyse en composantes principales est faite. Les images obtenues montrent clairement les effets de l'anisoplanétisme et l'évolution temporelle de la turbulence.

Key words: Image processing, Infrared atmospheric propagation, Atmospheric turbulence, Principal component analysis, Image sequence, Simulation, Time variation.

Contents

I. INTRODUCTION

This paper deals with the simulation of high-resolution images degraded by atmospheric turbulence. Atmospheric turbulence perturbs the optical propagation and therefore severely limits the observation of objects lying far away from the optical system. This is the case in astronomy, or for ground-to-ground vision over several tens of kilometers [1]. The real capture of these kinds of high-resolution images implies the use of an expensive and advanced optical system, hence the interest of a simulation method allowing to produce these images under different atmospheric conditions. The research that has already been carried out in this field applies mainly to astronomical observations. It consists in simulating a wavefront which is at first plane, and is then perturbed by passing through turbulent atmospheric layers. The simulation is usually limited to the calculation of the wavefront phase [2,3]. However, Kouznetsov et al. [4] proposed a method for the simulation of two linked random phenomena, such as the phase and amplitude of a turbulent wavefront. All these simulations are developed for the isoplanatic case, for which the perturbation is the same across the whole field of view; but an algorithm modeling the anisoplanatism effects has been proposed by H. Beaumont [5].

We propose a method for the simulation of a short-exposure image sequence taken at a quite high sampling frequency in a less common case, that of horizontal propagation through turbulence, over a distance of roughly ten kilometers. These conditions present some noteworthy differences in comparison with those that are usually

*LE2I Laboratoire d'Électronique, d'Informatique et d'Image, Université de Bourgogne – Aile de l'Ingénieur – Bâtiment Mirande-Allée Alain Savary – Dijon – France, e-mail :cbondeau@u-bourgogne.fr, ebourenn@u-bourgogne.fr, paindav@u-bourgogne.fr

stated. First of all, the refraction index structure constant C_n^2 remains almost the same along the propagation path, because the atmospheric layers are horizontally stratified. Secondly, the images very often show an obvious anisoplanatic character, because the field of view is wider than for astronomical observation. Finally, since turbulence fluctuates with time, the images of a given sequence present more or less similarities, depending on the sampling frequency. Therefore, the temporal behaviour of the turbulence has to be taken into account in the simulation.

In the first part of this paper, we explain the simulation method for degraded images taken at fairly wide time intervals, in the case of total anisoplanatism, and which is based on the works cited above. In the second part, we show how, starting from what is known about the temporal evolution of turbulence, and using principal component analysis (PCA), we can build up a whole sequence of degraded images at a fixed sampling frequency.

II. TURBULENCE-DEGRADED IMAGE SIMULATION

Atmospheric turbulence is due to the random motion of air masses at various temperatures, that provokes local fluctuations of the air refraction index value. Figure 1 shows the effects of these fluctuations on a wave issued from a star : this wave, plane at the entrance of the atmosphere, is distorded because of its passage through the atmosphere. Thus, a plane wave propagating through a turbulent medium undergoes amplitude and phase variations that follow known statistic laws [1].

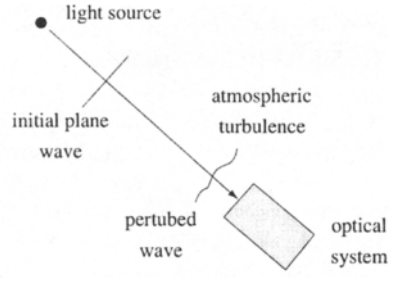

FIG. 1. — Propagation through turbulence

Propagation à travers la turbulence

In particular, the Kolmogorov's law says that the phase fluctuation power spectrum W_φ is proportional to $f^{-11/3}$, f being the spatial frequency amplitude. The simulation of a turbulent wavefront is often limited to the calculation of its phase $\varphi(r)$, because the amplitude fluctuations are usually negligible, compared with those of the phase [1]. The wavefront Ψ can thus be written :

$$\Psi(r) = exp[j\varphi(r)], \tag{1}$$

$r = (x, y)^T$ representing the point of (x, y) coordinates in a plane perpendicular to the direction of propagation of the wave. One of the first simulation methods was proposed by B. L. McGlamery [2]. It consisted in generating a random variable as the phase Fourier transform, and then in multiplying it by $f^{-11/6}$, so that the phase fluctuation power spectrum follows the Kolmogorov law. The problem of this frequential filtering is that it underestimates low frequencies. We chose then to start from the method proposed by N. Roddier [3] : the phase $\varphi(r)$ being decomposed on a Zernike polynomial base [6,7], a random draw law allows to generate the expansion coefficients, so that the wavefront follows the commonly used Kolmogorov's turbulence model.

The atmospheric impulse response (or point-spread function) h is the image formed by the point-source emitting the wavefront Ψ. It is given by the squared Fourier transform modulus of the received incident wavefront part :

$$h(\beta) = |\mathcal{F}[P(r)\Psi(r)]|^2, \tag{2}$$

$P(r)$ being the pupil function, that equals 1 inside the optical system pupil and 0 outside, and $\mathcal{F}$ the Fourier transform operator ; β represents the angular observation direction. If we can consider that this impulse response is spatially invariant across the field of view θ, the image i of an object o is given by :

$$i(\alpha) = \int_\theta h(\alpha - \beta)o(\beta)\mathrm{d}\beta. \tag{3}$$

Actually, since the atmospheric turbulence is widely distributed in space, the wavefront perturbations are not identical for all wavefront directions. In this case, called anisoplanatic case, the point-spread function is not the same for all points of the image [1]. In order to simulate anisoplanatism, we integrated the method developed by H. Beaumont [5] : the atmospheric impulse response, depending on the observation direction, can be simulated according to the following formula :

$$h(\beta, \beta') = |\mathcal{F}[P(r - \ell\beta')\Psi(r)]|^2 \tag{4}$$

and the image is then linked to the object by :

$$i(\alpha) = \int_\theta h(\beta, \beta - \alpha)o(\beta)\mathrm{d}\beta. \tag{5}$$

This is the same as considering a single turbulent layer of dimensions larger than those of the pupil, and as selecting a different part of it for each image pixel, by moving the pupil across the wavefront. The parameter ℓ allows to control the impulse response correlation degree between two adjacent points.

Case of total anisoplanatism

We propose here an extension of the simulation to a total anisoplanatism case. We call "total anisoplanatism" the case for which the angular pixel resolution is greater than the isoplanatism angle, and thus for which each pixel is in principle decorrelated from its neighbours. Theoreti-

cally, the maximum decorrelation between the images of two point sources separated by Δp pixels will be obtained for $\ell \Delta p \geq D$: the wavefront parts that are used in the calculation of their respective responses are thus not connected. Consequently, for a $N \times N$ pixel image, we need to generate a ND-diameter circular wavefront. For example, for a 40×40 pixel object and a 32-element diameter pupil (a common case in our simulation), the wavefront to be calculated should have a dimension of the order of 1280×1280 elements. This poses a problem of memory size and computation time (several hours for a single image simulation).

However, if we take for the object two point sources s_1 and s_2 separated by the camera's resolution angle, and compute the correlation rate between the two responses i_1 and i_2 lying in the image for different values of D/r_0 and ℓ (again with $D = 32$ elements), we observe (Fig. 2) that it reaches its limiting value faster than expected, i.e. before $\ell = D = 32$; the limiting value depends on the ratio D/r_0, r_0 being the Fried parameter [8]. In particular, for $D/r_0 = 3$, we see that the correlation rate stabilizes from $\ell \cong 15$ upwards. Choosing ℓ between 15 and 32, we can thus generate a smaller wavefront (with a diameter from 0. 5 ND to ND elements). In the simulations presented in the following of this paper, we chose $\ell = 18$, in order to place ourselves in the total anisoplanatism case.

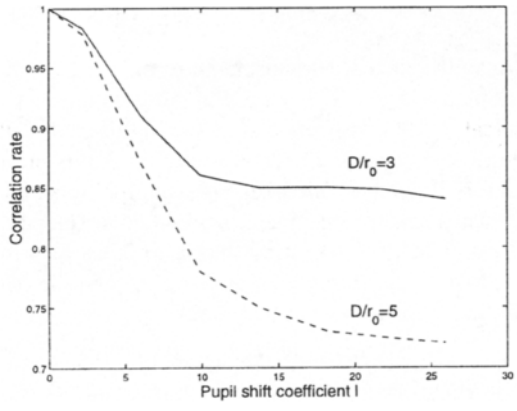

FIG. 2. — Correlation rate between the images of two neighbouring source points versus ℓ

Taux de corrélation entre les images de deux points sources voisins en fonction de ℓ

The original image used in our simulations is in Figure 3. We reproduce here the type of observations that can be realized with an infrared imaging system, either in 3-5 or 8-12 μm wavelength intervals. In order to simulate a high temperature difference between the object and the background, we chose a binary image. However, this simulation could be done in visible light, since the wavelength λ appears in the expression of the Fried parameter [1]:

$$r_0 = [0{,}423\, L(2\pi/\lambda)^2 C_n^2]^{-3/5} \tag{6}$$

in the case of horizontal propagation along a distance L ; C_n^2 is the structure parameter of the refractive index fluctuations, characterizing the turbulence strength, and depends on the meteorological conditions.

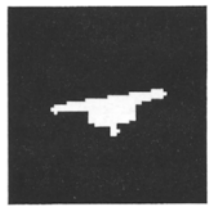

FIG. 3. — Original binary image

Image binaire initiale

We present in Figure 4 some simulations realized with a 32-element pupil along its diameter, $\ell = 18$ and $D/r_0 = 3$; we are thus here in the case of total anisoplanatism. The images were saturated at the output. We can observe various deformations, especially at the tips of the object.

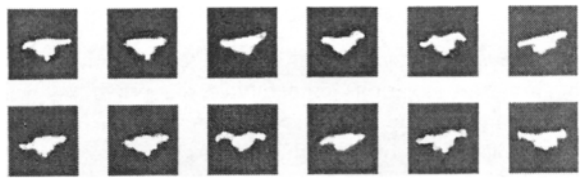

FIG. 4. — Short-exposure images, total anisoplanatism

Images en pose courte et anisoplanétisme total

We note that the deformations vary across the images, because of the anisoplanatism effect. These degraded images are temporally decorrelated from each other, since each coefficient set representing a phase sample is chosen randomly, and is independent from the other samples. In order to simulate a sequence of images captured at short intervals, we have to take into account the way in which turbulence evolves over time. This point is addressed in the following section.

III. SIMULATION OF A TURBULENCE-DEGRADED IMAGE SEQUENCE

To simulate a whole sequence of short-exposure images, we have to take into account the temporal turbulence fluctuations, which last a few milliseconds. If we capture these images at shorter time intervals, they will show a certain correlation. Here we adopt the filtering principle of B. L. McGlamery's simulation [2], but apply it to the wavefront phase temporal spectrum.

III.1. Initial data

Following N. Roddier's method, we can generate N phase samples φ_n, $n = 1,\ldots, N$, each represented by its first $K - 1$ decomposition coefficients[1] set as column vectors $\boldsymbol{a}_n = [a_{2n} \ldots a_{Kn}]^T$. N. Roddier starts from the theoretical covariance matrix $\boldsymbol{W}$ of the coefficients to generate the phase samples. The values of the $\boldsymbol{W}$ matrix are given by Noll [6]. As for us, we used 4096 such samples that were calculated by the ONERA. These samples are temporally decorrelated from each other; they do not follow any temporal evolution law. If we store these N column vectors $\boldsymbol{a}_n$ side by side in a randomly way in a matrix $\boldsymbol{A}$ of dimensions $(K - 1) \times N$, we obtain :

$$(7) \quad \boldsymbol{A} = \begin{bmatrix} a_{21} & a_{22} & \ldots & a_{2n} & \ldots & a_{2N} \\ \vdots & \vdots & & \vdots & & \vdots \\ a_{j1} & a_{j2} & \ldots & a_{jn} & \ldots & a_{jN} \\ \vdots & \vdots & & \vdots & & \vdots \\ a_{K1} & a_{K2} & \ldots & a_{Kn} & \ldots & a_{KN} \end{bmatrix},$$

where a_{jn} is the j-th order coefficient of the n-th sample phase φ_n, represented by the $\boldsymbol{a}_n$ column vector. Each row vector of A is formed by the N Zernike coefficients of a given order j and constitutes a white noise :

$$(8) \quad E[a_{jp}\, a_{jq}] = E[a_j^2]\delta(p, q),$$

where p and q are integers between 1 and N, $E[\ ]$ is the mean operator and $\delta(p, q)$ is the Kronecker symbol. As examples, Figure 5 shows the different values of a_{2n}, a_{3n} and a_{4n} $(n = 1,\ldots, N)$.

The structure function of the phase φ is defined by :

$$(9) \quad \mathcal{D}_\varphi(\rho) = \langle |\varphi(\boldsymbol{r}) - \varphi(\boldsymbol{r} + \rho)|^2 \rangle.$$

In the case of a Kolmogorov turbulence, $\mathcal{D}_\varphi$ is theoretically such that [8] :

$$(10) \quad \mathcal{D}_\varphi(\rho) = 6.88(\rho/r_0)^{5/3},$$

where $\rho = |\rho|$. We see (Fig. 6) that the structure function $\mathcal{D}_\varphi(\rho/r_0)$ (continuous line), realized from 100 phase samples, is very close to the theoretical curve (dotted line).

We use these data as the starting point of the construction of a sample sequence.

1. a_1 is the piston mode coefficient (average phase), useless for the simulation.

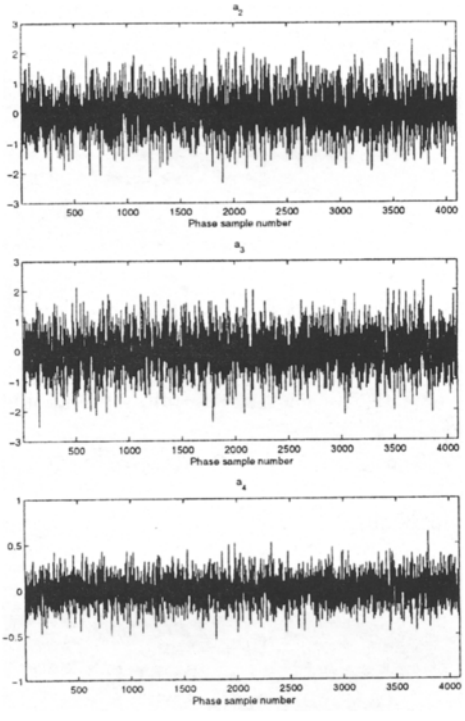

FIG. 5. — Simulated Zernike coefficients (a_2, a_3, a_4)

Coefficients de Zernike simulés (a_2, a_3, a_4)

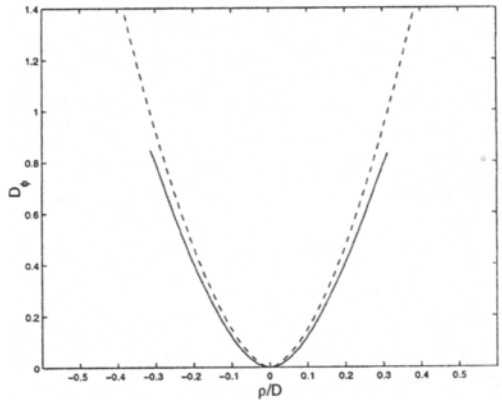

FIG. 6. — Simulated phase structure function

Simulation de la fonction de structure des phases

III.2. Temporal evolution of the turbulent wavefront phase

To simulate an image sequence consists in simulating a turbulent wavefront sequence, that is to say, a turbulent wavefront phase sequence. The phase is expressed as a decomposition on a Zernike polynomial base :

$$(11) \quad \varphi(\boldsymbol{r}, t) = \sum_{j=2}^{K} a_j(t)\, Z_j(\boldsymbol{r}).$$

The aim is finally to obtain a time-dependent coefficient sequence forming a set of S data, each described by its K-1 components, as indicated hereafter :

(12)
$$\begin{array}{cc} & \text{time} \\ & a_2(t)\ a_2(t+\Delta t)\ a_2(t+2\Delta t)\ \ldots\ a_2(t+(S-1)\Delta t) \\ \text{data components} & \vdots\quad\ \vdots\quad\ \vdots\qquad\ \vdots \\ & a_K(t)\ a_K(t+\Delta t)\ a_K(t+2\Delta t)\ \ldots\ a_K(t+(S-1)\Delta t) \end{array}$$

Δt corresponding to the time interval between two image captures, and S to the number of images needed for the sequence. Each j-th row vector of this matrix must follow the theoretic temporal evolution of each $a_j(t)$ coefficient, and simultaneously, each n-th column vector $\boldsymbol{a}_n$ $(n = 0,\ldots, S-1)$ must define a phase that obeys the Kolmororov's law.

We use hereafter the following notations : ν stands for the temporal frequency, and $\boldsymbol{f} = (f_x, f_y)$ is the spatial frequency, with modulus $f = \sqrt{(f_x^2, f_y^2)}$.

The temporal power spectrum of the turbulent wavefront phase coefficients depends on wind direction and speed. Here, let us suppose that the wind speed V is oriented along the x axis (the simulation principle can be extrapolated later to any direction). The theoretical temporal power spectrum for a coefficient a_j at a given order j is then written [9] :

$$w_j(\nu) = \frac{1}{V}\int_{-\infty}^{\infty}\left|\tilde{M}_j\left(\frac{\nu}{V}, f_y\right)\right|^2 W_\varphi\left(\frac{\nu}{V}, f_y\right) \mathrm{d}f_y. \tag{13}$$

In the above equation, W_φ stands for the phase spatial power spectrum. For a plane wave propagating through the atmosphere along a distance L, in the case of a Kolmogorov turbulence, it is given by [1] :

$$W_\varphi(\boldsymbol{f}) = W_\varphi(f_x, f_y) = 0.033\,(2\pi)^{-2/3}(2\pi/\lambda)^2 f^{-11/3}\int_0^L C_n^2(h)\ \mathrm{d}h, \tag{14}$$

where λ is the wavelength. The structure constant C_n^2 of the refractive index fluctuations depends only on the altitude. Therefore, in the case of horizontal propagation along a distance L, C_n^2 is constant, which gives :

$$W_\varphi(\boldsymbol{f}) = 0.033\,(2\pi)^{-2/3}(2\pi/\lambda)^2 L f^{-11/3} C_n^2. \tag{15}$$

Taking Eq. (6) into account, we can simplify this expression by introducing r_0:

$$W_\varphi(\boldsymbol{f}) = 0.023\, r_0^{-5/3} f^{-11/3}, \tag{16}$$

and Eq. (13) becomes :

$$w_j(\nu) = \frac{0.023\, r_0^{-5/3}}{V}\int_{-\infty}^{\infty}\left|\tilde{M}_j\left(\frac{\nu}{V}, f_y\right)\right|^2 \left(\left|\frac{\nu}{V}\right|^2 + f_y^2\right)^{-11/6} \mathrm{d}f_y. \tag{17}$$

2. The number j of a considered polynomial is related to m and n by : $n = IP\left[(\sqrt{8j-7}-1)/2\right]$

$$m = \begin{cases} 1 + 2IP\left\{\left|j - 1 - IP\left[n(n+1)/2\right]\right|/2\right\} & \text{if } n \text{ odd} \\ 2IP\left\{\left|j - IP\left[n(n+1)/2\right]\right|/2\right\} & \text{if } n \text{ even} \end{cases} \tag{18}$$

IP = integer part

Finally, $\tilde{M}j\ (f)$ is the Fourier transform of the j-th Zernike polynomial. For a given Z_{nm} polynomial[2] (n = radial degree, m = azimutal frequency), its module can be written [6] :

$$|\tilde{M}_j(f)| = \sqrt{n+1}\,\frac{2|J_{n+1}(\pi D f)|}{\pi D} \begin{cases} \left|\sqrt{2}\right|\cos(m\theta)| & \text{if } j \text{ even} \\ \left|\sqrt{2}\right|\sin(m\theta)| & \text{if } j \text{ odd} \end{cases} \quad \text{for } m \neq 0 \tag{19}$$
$$1 \quad \text{for } m = 0.$$

III.3. Phase sample sequence construction

First of all, we construct a set of random variables whose power spectrum corresponds to the theoretical temporal spectrum of the Zernike coefficients at different orders. To do this, $K-1$ numerical Gaussian white noise signals $x_j(t)$, $\{j = 2,\ldots, K\}$ are generated, with the same characteristics, at a given order j, as those of the original coefficients : zero average, variance $\sigma_j^2 = a_j^2$. Then, for each j, we filter the power spectrum $|\tilde{x}_j(\nu)|^2$ of the $x_j(t)$ signals with the normalized-density power spectrum $w_j(\nu)$ of each coefficient a_j, and we call $\tilde{y}_j(\nu)$ the square root of the filtered power spectrum thus obtained :

$$\tilde{y}_j(\nu) = |\tilde{x}_j(\nu)|\,|w_j(\nu)|^{1/2}. \tag{20}$$

We put the signals $y_j(t)$, set as row vectors $\boldsymbol{y}_j$, together in a $(K-1)\times S$ matrix (S being the number of $y_j(t)$ signal samples) :

$$\boldsymbol{Y} = \begin{bmatrix} \boldsymbol{y}_2 \\ \vdots \\ \boldsymbol{y}_K \end{bmatrix} \tag{21}$$

Each row vector of $\boldsymbol{Y}$ represents a possible temporal evolution of the corresponding Zernike coefficient ; but the phase samples that can be built with each column vector of $\boldsymbol{Y}$ do not necessarily follow the Kolmogorov turbulence model.

Let us consider now $\boldsymbol{A}$ matrix, where each column vector $\boldsymbol{a} = [a_2 \ldots a_K]^{\mathrm{T}}$ representing one of the N initial time-independent phase samples has been normalized (see paragraph III. 1). We calculate $\boldsymbol{W}$, the covariance matrix of these data :

$$\boldsymbol{W} = \frac{\boldsymbol{A}\boldsymbol{A}^{\mathrm{T}}}{N}. \tag{22}$$

Each element of $\boldsymbol{W}$ matrix is then given by :

$$W_{i,j} = \mathrm{E}\,|a_i\, a_j|. \tag{23}$$

The singular value decomposition of $\boldsymbol{W}$ gives Δ, the matrix of $\boldsymbol{W}$ eigenvalues, ordered in a decreasing manner, and $\boldsymbol{P}$, the corresponding eigenvector matrix, such as :

$$\boldsymbol{W} = \boldsymbol{P}\Delta\boldsymbol{P}^{\mathrm{T}}. \tag{24}$$

The eigenvectors are called principal axes of the data; the first of them indicate the directions of the largest variances of our time-independent data. The projection of $\boldsymbol{Y}$ matrix onto these axes is defined by :

$$\boldsymbol{Z} = \boldsymbol{P}^{\mathrm{T}}\boldsymbol{Y}. \tag{25}$$

Each column vector of $\boldsymbol{Z}$ matrix thus contains the coordinates of the corresponding coefficient column vector of $\boldsymbol{Y}$ in the system formed by the principal axes.

The covariance matrix of $\boldsymbol{Z}$ is given by :

$$\frac{\boldsymbol{Z}\boldsymbol{Z}^{\mathrm{T}}}{S} = \frac{\boldsymbol{P}^{\mathrm{T}}\boldsymbol{Y}\boldsymbol{Y}^{\mathrm{T}}\boldsymbol{P}}{S} = \boldsymbol{P}^{\mathrm{T}}\boldsymbol{W}_{\boldsymbol{Y}}{}^{\mathrm{T}}\boldsymbol{P}. \tag{26}$$

Assuming that the coefficient sequences of $\boldsymbol{Y}$ follow the Kolmogorov turbulence model, they should have the same covariance matrix as the initial data :

$$\boldsymbol{W}_{\boldsymbol{Y}} = \frac{\boldsymbol{Y}\boldsymbol{Y}^{\mathrm{T}}}{S} = \boldsymbol{W}, \tag{27}$$

which implies :

$$\frac{\boldsymbol{Z}\boldsymbol{Z}^{\mathrm{T}}}{S} = \boldsymbol{P}^{\mathrm{T}}\boldsymbol{W}\boldsymbol{P} = \Delta. \tag{28}$$

The covariance matrix of $\boldsymbol{Z}$ should be diagonal, with its diagonal elements equal to the eigenvalues of $\boldsymbol{W}$.

A means of recognizing correct sequences is therefore to calculate the following distance :

$$d = \left\| \frac{\boldsymbol{Z}\boldsymbol{Z}^{\mathrm{T}}}{S} - \Delta \right\|. \tag{29}$$

We use this quantity as a criterion to operate a selection on our simulated sample sequences : those that give the minimum distance are the closest to the Kolmogorov turbulence model. We obtain this way sample sequences both temporally correlated and spatially in accordance with the turbulence statistics.

III.4. Verifications

The simulated wavefronts must follow the Kolmogorov turbulence model. We can verify this by examining the phase structure function $\mathcal{D}_{\varphi}$, which definition and theoretical expression are given in Eq. (9) and (10). Figure 7 shows the structure function curve, calculated starting from 300 phase samples coming from 100 different sequences (continuous line). We can see that this curve is close to the theoretical one (dashed line). Thus the simulation closely reproduces the turbulence effects on a wavefront.

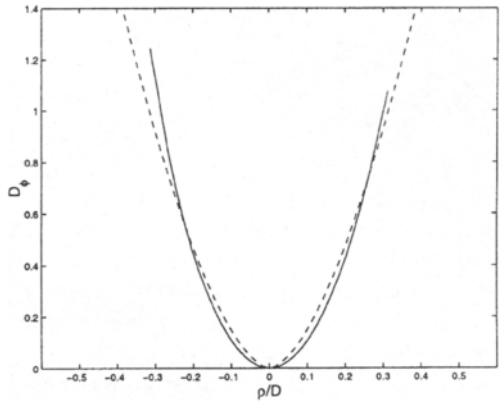

FIG. 7. — Simulated structure function of phase sequences

Simulation de la fonction de structure des séquences de phases

III.5. Examples

Figure 8 shows 4 image sequences obtained in the manner explained above. We can clearly see that the object image evolves. The conditions here are : $V = 6\ \mathrm{ms}^{-1}$, $D/r_0 = 3$ and $\Delta t = 0.25$ s, that is, a sampling frequency of 4 Hz.

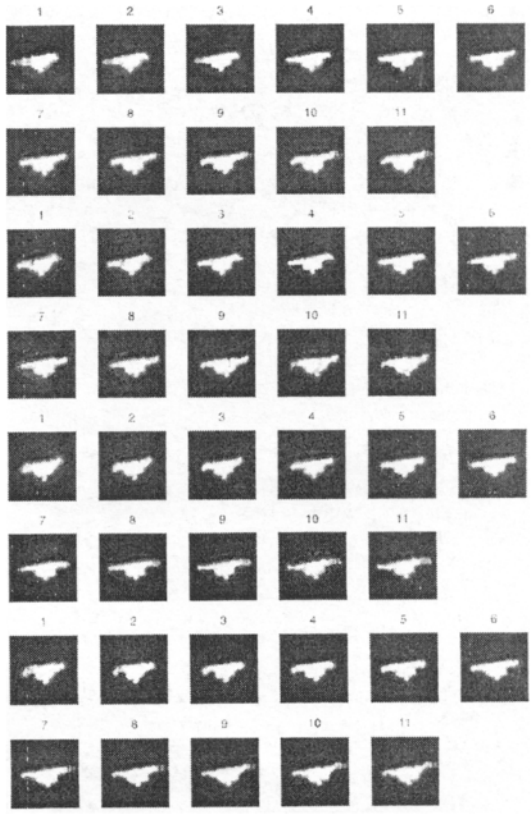

FIG. 8. — 4 image sequences ($D = 3r_0$)

4 séquences d'images ($D = 3r_0$)

IV. CONCLUSION

We presented a simulation method of high-resolution images degraded by atmospheric turbulence in the anisoplanatic case. The simulation was at first used for images taken at fairly wide time intervals, and consequently temporally decorrelated from each other; then it was extended to a whole image sequence for a given sampling frequency. The accordance of the simulation with the Kolmogorov turbulence model is shown. This simulation is very useful when we want to study the turbulence effects on high-resolution image capture, but when suitable equipment is not available. Moreover, the work that was developed here in the infrared case can also be applied to the case of visible light. These results can also help with predictions when a further restoration is planned.

Acknowledgements

We would like to thank J.-M. Conan and V. Michau from the ONERA (France) for helping us with the generation of Zernike expansion coefficients.

This work is partially supported by the Conseil Régional de Bourgogne and SFIM Industries.

Manuscrit reçu le 8 décembre 1998
Accepté le 8 mars 1999

REFERENCES

[1] RODDIER (F.). Progress in optics XIX. Chapt. 5 : The effects of atmospheric turbulence in optical astronomy, *E. Wolf, North-Holland Publishing Company, Amsterdam*, pp. 281-376, (1981).

[2] MCGLAMERY (B.-L.). Computer simulation studies of compensation of turbulence degraded images, *Proc. of SPIE Conf. on Image Processing*, **74**, pp. 225-233, (1976).

[3] RODDIER (N.). Atmospheric wavefront simulation using Zernike polynomials. Opt. Eng, **29**, n° 10, pp. 1174-80, (1990).

[4] KOUZNETSOV (N.), VOITSEKHOVICH (V. V.), ORTEGA-MARTINEZ (R.). Simulations of turbulence-induced phase and log-amplitude distorsions, *Appl. Opt.* **36**, n° 2, pp. 464-469, (1997).

[5] BEAUMONT (H.). Caractérisation de la turbulence atmosphérique et procédure d'amélioration des images pour des observations horizontales au-dessus de la mer, *PhDthesis*, (1996).

[6] NOLL (R. J.). Zernike polynomials and atmospheric turbulence, *J. Opt. Soc. Am.*, **66**, n° 3, pp. 207-211, (1976).

[7] FRIED (D. L.). Statistics of a geometric representation of wavefront distorsion, *J. Opt. Soc. Am.*, **55**, n° 11, pp. 1427-1435, (1965).

[8] FRIED (D. L.). Optical resolution through a randomly inhomogeneous medium for very long and very short exposures, *J. Opt. Soc. Am.*, **56**, n° 10, pp. 1372-1379, (1966).

[9] CONAN (J.-M.), ROUSSET (G.), MADEC (P.-Y.). Wavefront temporal spectra in high resolution imaging through turbulence, *J. Opt. Soc. Am.*, **12**, pp. 1559-1570, (1995).

BIOGRAPHIES

Christine BONDEAU has received the DEA in Physics from the University of Burgundy in June 1994 and is currently working towards her PhD at the LE2I. She works in the area of image processing.

El-Bay BOURENNANE received the PhD degree in automatics and image processing from the University of Burgundy in 1994, at the LE2I. He is currently teacher-cum-researcher at the University of Burgundy. His research interests are mainly in image processing.

Michel PAINDAVOINE received a PhD in electronics and signal processing at Montpellier University, France, 1982. He is currently full Professor and member of LE2I, Laboratory of Electronics, Computer, and Imaging Sciences, Université de Bourgogne, France. His main research topic is real time image processing.